EMP Interaction Notes

Note IX

QUASISTATIC MAGNETIC FIELD TRANSMISSION THROUGH CIRCULAR APERTURES

17 JULY 1967

JOHN N. BOMBARDT, JR.

ELECTROMAGNETIC EFFECTS BRANCH
U.S. ARMY ENGINEER RESEARCH AND DEVELOPMENT LABORATORIES

ABSTRACT

1.
Kaden's quasistatic analysis of a circular aperture in a conducting plane is reviewed and the field components of interest are obtained. The numerical results of Kaden's theory are correlated with the experimental data obtained for an interior field component within an open-ended, long cylinder with circular cross-section and with a circular aperture on the lateral surface. The single aperture numerical results obtained from Kaden's theory incorporate more terms in the series solution than the
2.
results obtained in an earlier note. Quasistatic analysis of multi-aperture problems is discussed and the approximation of linear superposition of independent solutions for a double aperture problem is made and numerical results obtained. These numerical results are correlated with experimental data obtained for an interior field component due to two circular apertures on the lateral surface of a cylinder.

I. SINGLE APERTURE THEORY

Consider a plane shield of infinite extent which is vanishingly thin and of infinite conductivity with a circular aperture of radius r_o. We employ spherical coordinates r, θ, φ with an origin located at the center of the aperture. In the upper space, $\theta > \pi/2$, we consider a magnetic field of strength H_o oriented parallel to the plane of the shield as shown below in Figure (1):

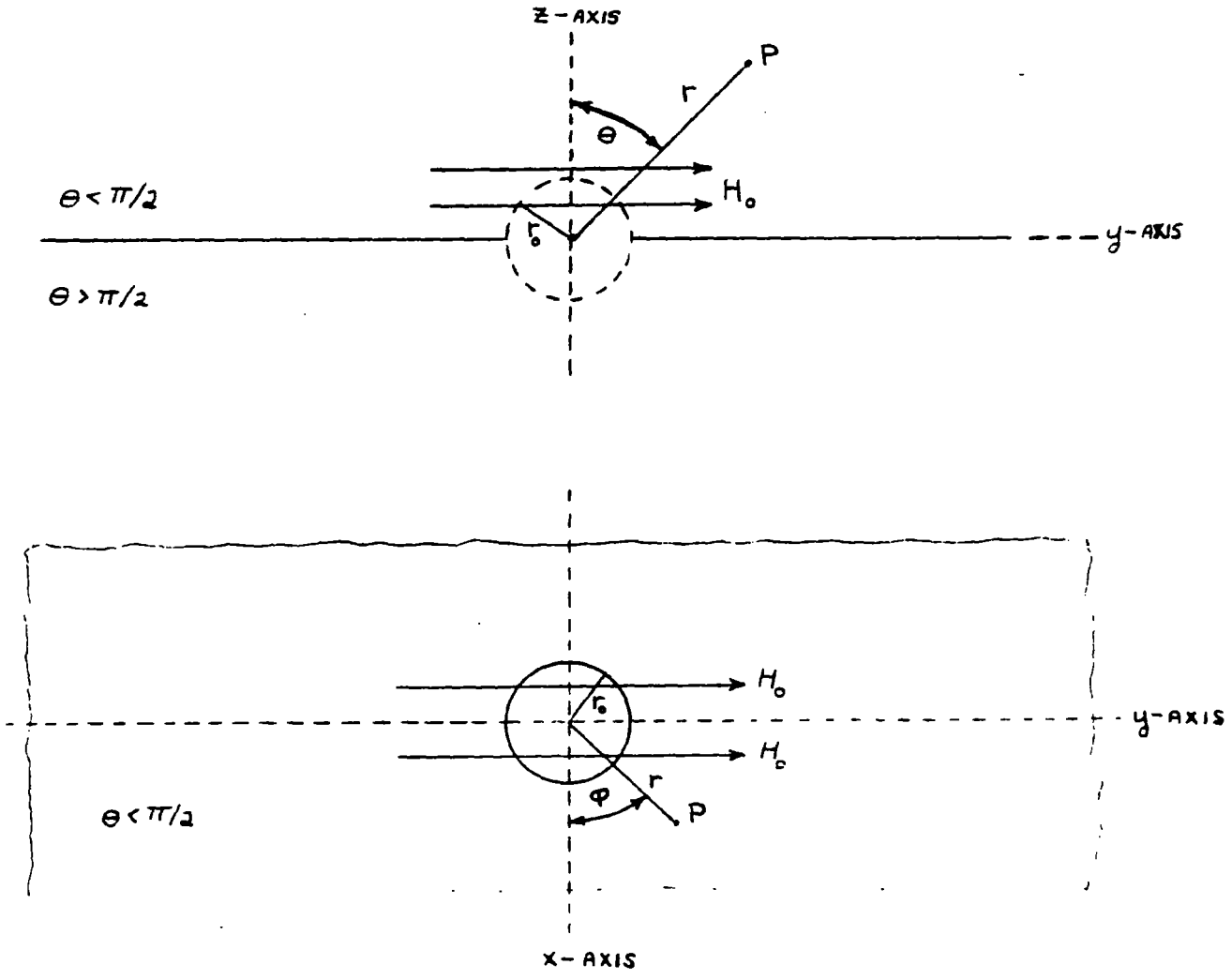

FIGURE (1)

The problem then is to calculate the magnetic field in the lower half-space, $\theta > \pi/2$. Kaden has solved this problem in the manner indicated below.

In the quasistatic or long wavelength approximation, the magnetic field can be derived from a magnetic scaler potential.

We have then

(1) $\bar{H} = \bar{\nabla} \phi_m$

The boundary conditions for the problem are given by

(2) $\left(\frac{\partial \phi_m(\bar{r})}{\partial \theta} \right)_{\theta = \pi/2} = 0 \qquad r \geq r_0$

(3) $\lim_{r \to \infty} \phi_m(\bar{r}) = H_0 r \sin\theta \sin\varphi \qquad 0 < \theta < \pi/2$

(4) $\lim_{r \to \infty} \phi_m(\bar{r}) = 0 \qquad \pi/2 < \theta < \pi$

In the upper half-space, $\theta < \pi/2$, a solution is assumed of the form given by

$$\phi_m(\bar{r}) = H_o r \sin\theta \sin\varphi + \sin\varphi \sum_{n=1,3,5,\ldots}^{\infty} \frac{A_m}{r^{m+1}} P_m'(\cos\theta) \quad , r > r_o \, , \theta < \pi/2 , \tag{5}$$

and in the lower half-space, $\theta > \pi/2$, a solution is assumed of the form given by

$$\phi_m(\bar{r}) = -\sin\varphi \sum_{n=1,3,5,\ldots}^{\infty} \frac{A_m}{r^{m+1}} P_m'(\cos\theta) \quad , r > r_o \, , \pi/2 < \theta < \pi . \tag{6}$$

Using the boundary conditions, Kaden evaluates the constant A_m , the calculation of which will not be repeated here, for the upper and lower half-spaces and for the "hole-sphere" region in which $r \leq r_o$. The potential solutions are found to be:

$$\phi_m(\bar{r}) = H_o r \sin\theta \sin\varphi$$

(7)
$$- \frac{2H_o r_o \sin\varphi}{\pi} \sum_{m=1,3,5,\ldots} \frac{(-1)^{(m-1)/2}}{m(m+2)} \left(\frac{r_o}{r}\right)^{m+1} P_m^1(\cos\theta), \; r > r_o \; ; \; \theta < \pi/2$$

$$\phi_m(\bar{r}) = H_o r \sin\varphi \left[\frac{1}{2}\sin\theta\right.$$

(8)
$$\left. + \frac{2}{\pi} \sum_{m=2,4,6,\ldots} \frac{(-1)^{m/2}}{(m^2-1)} \left(\frac{r}{r_o}\right)^{m-1} P_m^1(\cos\theta)\right], \; r \leq r_o \; ,$$

(9) $$\phi_m(\bar{r}) = -\frac{2H_o r_o \sin\varphi}{\pi} \sum_{m=1,3,5,\ldots}^{\infty} \frac{(-1)^{(m-1)/2}}{m(m+2)} \left(\frac{r_o}{r}\right)^{m+1} P_m^1(\cos\theta), \; r > r_o \; ; \; \frac{\pi}{2} < \theta < \pi .$$

In shielding theory we are primarily interested in the fields that penetrate the shield under consideration. Thus our interest lies in the "hole-sphere" region and lower-half space region in which we desire the magnetic field components. Secondly, most practical considerations of interest, in which the quasistatic approximation can be applied, are concerned with aperture radii which are smaller than field point distances where fields are to be calculated. In essence, then, we restrict our attention to the potential and field solutions in the lower-half spaces for which $r > r_o$ and $\pi/2 < \theta < \pi$ and for which equation (9) gives the magnetic scalar potential solution.

The desired field components in the region of interest are found to be

$$H_r = \frac{\partial \phi_m(\bar{r})}{\partial r}$$

(10)

$$= \frac{2H_o \sin\varphi}{\pi} \sum_{m=1,3,5,\ldots}^{\infty} \frac{(-1)^{(m-1)/2}(m+1)}{m(m+2)} \left(\frac{r_o}{r}\right)^{m+2} P_m^1(\cos\theta),$$

$$H_\theta = \frac{1}{r} \frac{\partial \phi_m(\bar{r})}{\partial \theta}$$

(11)

$$= -\frac{2H_o \sin\varphi}{\pi \sin\theta} \sum_{m=1,3,5,}^{\infty} \frac{(-1)^{(m-1)/2}}{m(m+2)} \left(\frac{r_o}{r}\right)^{m+2} \left[m\cos\theta\, P_m^1(\cos\theta) - (m+1) P_{m-1}^1(\cos\theta)\right],$$

$$H_\varphi = \frac{1}{r\sin\theta}\frac{\partial \phi_m(\bar{r})}{\partial \varphi}$$

(12)

$$= -\frac{2H_0\cos\varphi}{\pi\sin\theta}\sum_{m=1,3,5,\ldots}^{\infty}\frac{(-1)^{(m-1)/2}}{m(m+2)}\left(\frac{r_0}{r}\right)^{m+2}P_m^1(\cos\theta),$$

where (11) has been evaluated using formula 8.5.4 in the NBS Handbook of Mathematical Functions. The first few terms for each of the above field components become:

$$H_r = \frac{2H_0\sin\varphi}{\pi}\left\{-\frac{2}{3}\left(\frac{r_0}{r}\right)^3\sin\theta + \frac{1}{10}\left(\frac{r_0}{r}\right)^5(5\sin 3\theta + \sin\theta)\right.$$

(13)

$$\left. -\frac{9}{448}\left(\frac{r_0}{r}\right)^7(21\sin 5\theta + 7\sin 3\theta + 2\sin\theta) + \ldots\right\},$$

$$H_\theta = -\frac{2H_0 \sin\varphi}{\pi \sin\theta}\left\{-\frac{1}{3}\left(\frac{r_0}{r}\right)^3 \sin\theta\cos\theta\right.$$

$$+\frac{3}{15}\left(\frac{r_0}{r}\right)^5\left[\frac{3}{8}\cos\theta(5\sin 3\theta+\sin\theta)-2\sin 2\theta\right] \tag{14}$$

$$\left.-\frac{1}{56}\left(\frac{r_0}{r}\right)^7\left[\frac{15}{16}\cos\theta(21\sin 5\theta+7\sin 3\theta+2\sin\theta)\right.\right.$$

$$\left.\left.-3(7\sin 4\theta+2\sin 2\theta)\right]+\ldots\right\},$$

$$H_\varphi = -\frac{2H_0\cos\varphi}{\pi\sin\theta}\left\{-\frac{1}{3}\left(\frac{r_0}{r}\right)^3\sin\theta+\frac{1}{40}\left(\frac{r_0}{r}\right)^5(5\sin 3\theta+\sin\theta)\right.$$

$$\left.-\frac{3}{896}\left(\frac{r_0}{r}\right)^7(21\sin 5\theta+7\sin 3\theta+2\sin\theta)+\ldots\right\}. \tag{15}$$

In the experiments to be discussed, it is experimentally advantageous to measure Cartesian components of the magnetic field. To obtain the Cartesian components of the magnetic field we first express the Cartesian unit vectors in terms of the spherical unit vectors so that

$$\hat{\imath} = \hat{r}\sin\theta\cos\varphi+\hat{\theta}\cos\theta\cos\varphi-\hat{\varphi}\sin\varphi, \tag{16}$$

(17) $\hat{j} = \hat{r}\sin\theta\sin\varphi + \hat{\theta}\cos\theta\sin\varphi + \hat{\varphi}\cos\varphi$

(18) $\hat{k} = \hat{r}\cos\theta - \hat{\theta}\sin\theta$

and thus obtain directly

(19) $H_x = \hat{\imath}\cdot\bar{H} = H_r\sin\theta\cos\varphi + H_\theta\cos\theta\cos\varphi - H_\varphi\sin\varphi$

(20) $H_y = \hat{j}\cdot\bar{H} = H_r\sin\theta\sin\varphi + H_\theta\cos\theta\sin\varphi + H_\varphi\cos\varphi$

(21) $H_z = \hat{k}\cdot\bar{H} = H_r\cos\theta - H_\theta\sin\theta.$

After a little algebra given in the Appendix to this paper, the Cartesian components are found to be

$$H_x = \frac{2H_0 \sin\varphi\cos\varphi}{\pi}\left\{\sum_{m=1,3,5,\ldots}^{\infty}\frac{(-1)^{(m-1)/2}}{m(m+2)}\left(\frac{r_0}{r}\right)^{m+2}\left[P_m^1(\cos\theta)\left((m+1)\sin\theta\right.\right.\right.$$

(22)

$$\left.\left.\left.+\frac{1-m\cos^2\theta}{\sin\theta}\right)+\frac{(m+1)\cos\theta}{\sin\theta}P_{m-1}^1(\cos\theta)\right]\right\},$$

$$H_y = \frac{2H_0}{\pi}\left\{\sum_{m=1,3,5,\ldots}^{\infty}\frac{(-1)^{(m-1)/2}}{m(m+2)}\left(\frac{r_0}{r}\right)^{m+2}\left[P_m^1(\cos\theta)\left((m+1)\sin^2\varphi\sin\theta\right.\right.\right.$$

(23)

$$\left.\left.\left.-\frac{m\sin^2\varphi\cos^2\theta+\cos^2\varphi}{\sin\theta}\right)+(m+1)P_{m-1}^1(\cos\theta)\right]\right\},$$

$$H_z = \frac{2H_0\sin\varphi}{\pi}\left\{\sum_{m=1,3,5,\ldots}^{\infty}\frac{(-1)^{(m-1)/2}}{m(m+2)}\left(\frac{r_0}{r}\right)^{m+2}\left[(2m+1)\cos\theta P_m^1(\cos\theta)\right.\right.$$

(24)

$$\left.\left.-(m+1)P_{m-1}^1(\cos\theta)\right]\right\}.$$

The first few terms for each Cartesian component of the field are found to be,

$$H_x = \frac{2H_0 \sin\varphi\cos\varphi}{\pi}\left\{-\left(\frac{r_0}{r}\right)^3 \sin^2\theta\right.$$

$$-\frac{1}{5}\left(\frac{r_0}{r}\right)^5\left[\frac{1}{8}(5\sin 3\theta+\sin\theta)\left(4\sin\theta+\frac{1-3\cos^2\theta}{\sin\theta}\right)+4\cos^2\theta\right] \tag{25}$$

$$-\frac{1}{7}\left(\frac{r_0}{r}\right)^7\left[\frac{3}{128}(21\sin 5\theta+7\sin 3\theta+2\sin\theta)\left(6\sin\theta+\frac{1-5\cos^2\theta}{\sin\theta}\right)\right.$$

$$\left.\left.+\frac{3}{8}\cot\theta(7\sin 4\theta+2\sin 2\theta)\right]-\cdots\right\},$$

$$H_y = \frac{2H_0}{\pi}\left\{\frac{1}{3}\left(\frac{r_0}{r}\right)^3(\sin^2\varphi\cos^2\theta+\cos^2\varphi-2\sin^2\varphi\sin^2\theta)\right.$$

$$+\frac{1}{5}\left(\frac{r_0}{r}\right)^5\left[\frac{1}{8}(5\sin 3\theta+\sin\theta)\left(4\sin^2\varphi\sin\theta-\frac{3\sin^2\varphi\cos^2\theta+\cos^2\varphi}{\sin\theta}\right)+2\sin 2\theta\right] \tag{26}$$

$$+\frac{1}{7}\left(\frac{r_0}{r}\right)^7\left[\frac{-3}{128}(21\sin 5\theta+7\sin 3\theta+2\sin\theta)\left(6\sin^2\varphi\sin\theta-\frac{5\sin^2\varphi\cos^2\theta+\cos^2\varphi}{\sin\theta}\right)\right.$$

$$\left.\left.-\frac{3}{8}(7\sin 4\theta+2\sin 2\theta)\right]+\cdots\right\},$$

$$H_z = \frac{2H_0 \sin\Phi}{\pi}\left\{-\left(\frac{r_0}{r}\right)^3 \sin\theta\cos\theta + \frac{1}{5}\left(\frac{r_0}{r}\right)^5\left[\frac{7}{8}\cos\theta(5\sin 3\theta + \sin\theta) - 2\sin 2\theta\right]\right.$$

$$(27)\qquad -\frac{1}{7}\left(\frac{r_0}{r}\right)^7\left[\frac{33}{128}\cos\theta(21\sin 5\theta + 7\sin 3\theta + 2\sin\theta)\right.$$

$$\left.\left. -\frac{3}{8}(7\sin 4\theta + 2\sin 2\theta)\right] + \ldots\right\}.$$

II. SINGLE APERTURE EXPERIMENT - H_z

To verify Kaden's theory for a circular aperture we consider an experiment involving transient magnetic fields. A transient magnetic field is generated inside a solenoid, or coil, by feeding the solenoid with a current pulse supplied by a capacitive discharge system. The resulting axial magnetic field within the solenoid is relatively uniform and small test items within the solenoid are exposed to the axial field. Since any quasistatic approximation for shielding problems places wavelength restrictions on electromagnetic fields, we must first investigate the frequency content of the transient magnetic field within the solenoid discussed above.

Desired magnetic fields measured within a solenoid at the ERDL Experimental Facility correspond to a critically damped case with

amplitude A and rise time t as indicated in Figure (2):

FIGURE (2)

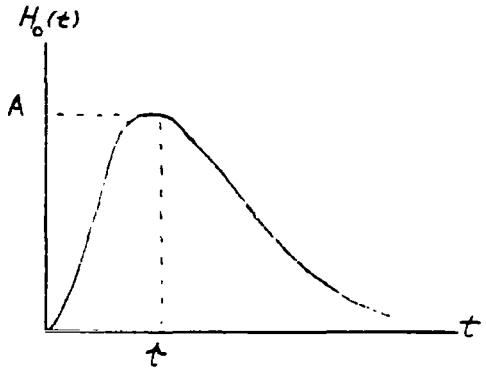

Analytically, then, the field can be approximated by the expression:

$$(28) \quad H_o(t) = \beta t e^{-\alpha t}$$

where β and α can be expressed in terms of the amplitude and rise time of the pulse. The critically damped case was implemented to obtain a magnetic field with the fastest rise time possible and yet with a reasonably large amplitude to facilitate measurement. The fastest rise time possible was used so that higher frequency components would be present to test the validity of the quasistatic approximation.

Setting the time derivative of $H_o(t)$ evaluated at $t = t$, equal to zero we obtain

$$\alpha = \frac{1}{t}$$

Similarly, setting $H_o(t)$ equal to A , we have

$$\beta = \frac{Ae}{t}$$

so that (28) becomes

$$H_o(t) = \frac{Ae}{t} t e^{-t/t} \tag{29}$$

To obtain the frequency spectrum of the field, we take Laplace transforms of (29) so that

$$\mathcal{L} H_o(t) = \frac{Ae}{t} \frac{1}{(s+1/t)^2} \tag{30}$$

Using $s = i\omega$, we have directly

$$|\mathcal{L} H_c(t)| = \frac{Aet}{\omega^2 t^2 + 1} \tag{31}$$

so that the normalized frequency spectrum is found from

$$\frac{|\mathcal{L} H_c(t)|}{Aet} = \frac{1}{\omega^2 t^2 + 1} \tag{32}$$

Equation (32) is plotted in Figure (3).

FIGURE (3)

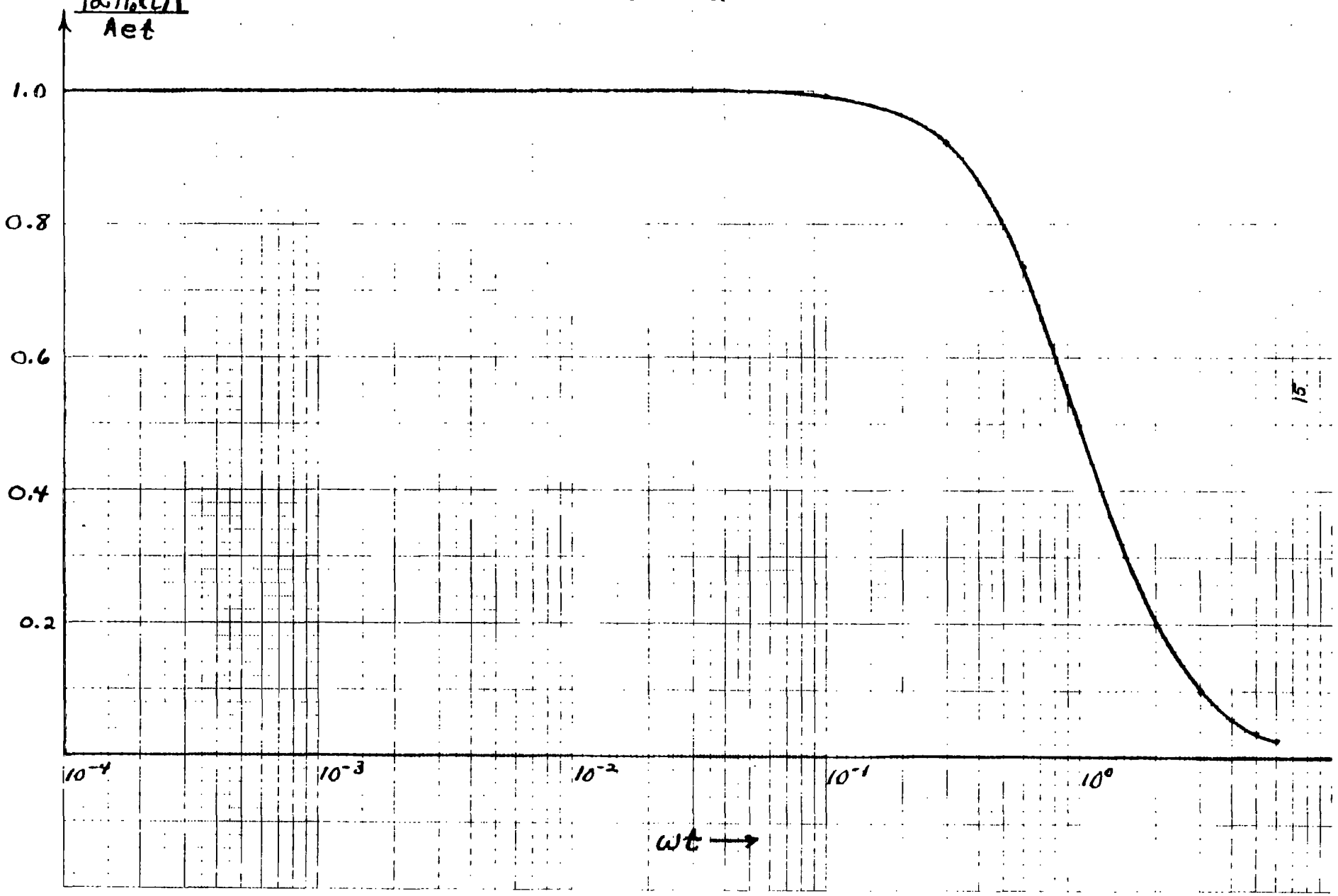
$\frac{|G H_0(t)|}{Aet}$
1.0
0.8
0.6
0.4
0.2
10^{-4}
10^{-3}
10^{-2}
10^{-1}
10^{0}
$\omega t \rightarrow$
15

From Figure (1), we note

$$\left| \frac{\mathcal{L} H_c(t)}{A e t} \right|_{\omega t = 3} = 0.1$$

so that the frequency spectrum of the solenoidal field is down 20 db at a value of

$$\omega = 3/t \tag{33}$$

For a rise time of $t = 10^{-6}$ seconds, the frequency spectrum of the field is thus down 20 db at an angular frequency of three megacycles or $f \approx 500 kc$. The corresponding wavelength at this frequency is about 600 meters and is necessarily longer for lower frequencies where most of the spectral energy occurs. With the characteristics of the main solenoid field specified, we now consider a particular experiment.

The most convenient geometry to employ for experiments within the solenoid are long hollow circular cylinders with open ends. The cylinders for the experiment discussed here are made of aluminum with an outside diameter of 33 centimeters. The thickness of the aluminum shell is approximately $3/16$ of an inch so that diffusion fields within the cylinder due to wall penetration of the external or main solenoid field are orders

of magnitude smaller than internal fields due to the penetration of the solenoid field through the aperture considered. The aperture introduced on the lateral surface of the cylinder is circular and of 10 centimeters in diameter.

The geometry and coordinates for the experiment performed are indicated below in Figure (4):

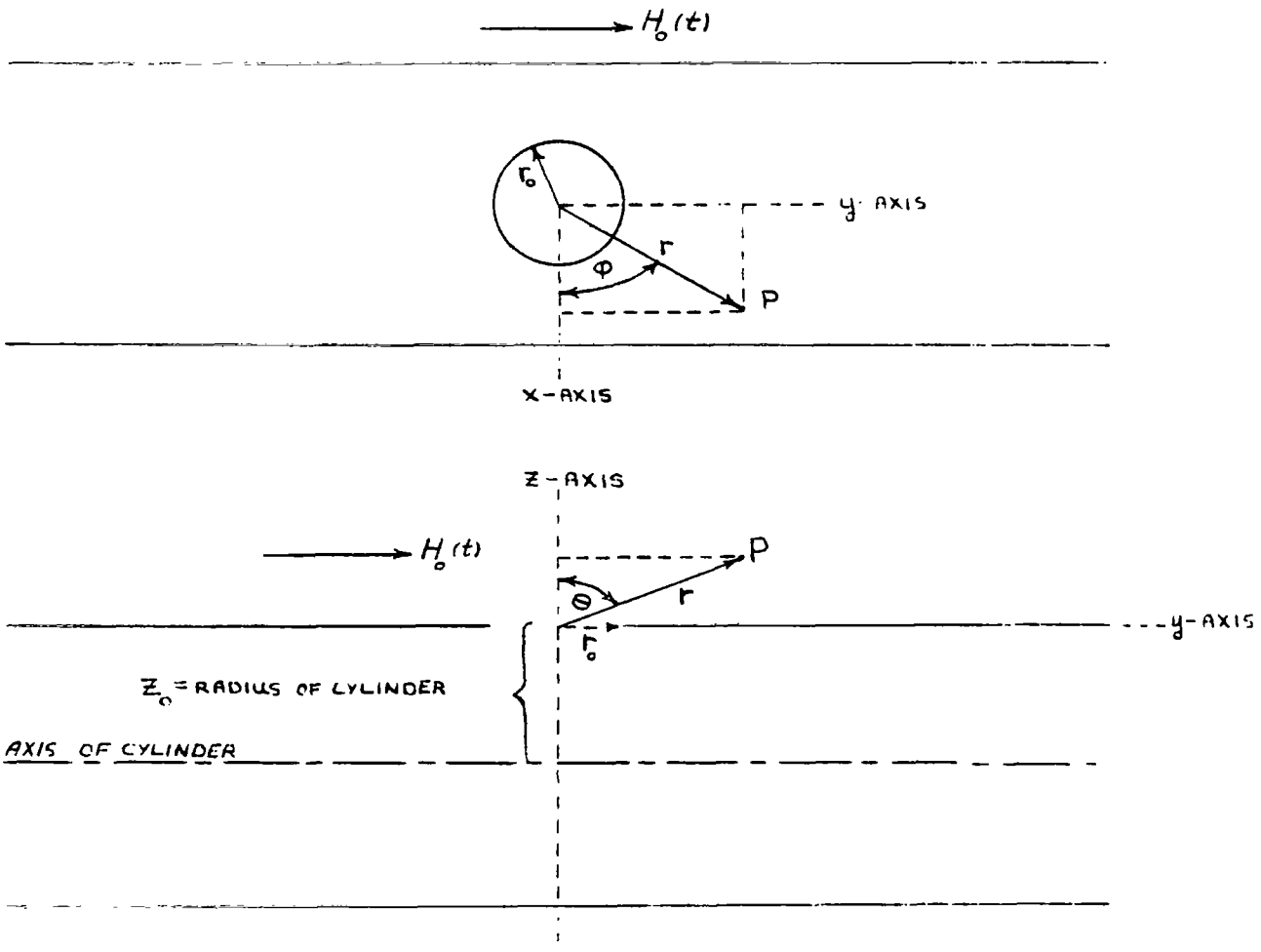

FIGURE (4)

Time history measurements were made of the $H_z(r,t)$ field inside the cylinder at points along the axis of the cylinder. As nearly as the oscillograms can be compared, the time history of the $H_z(r,t)$ measurements is the same as the time history for the external field, $H_c(t)$, produced by the solenoid in the absence of the cylinder with an aperture. Magnitude scaling of interior fields is now considered.

III. CORRELATION FOR A SINGLE APERTURE.

To compare Kaden's quasistatic theory with the results obtained in the previously described experiment for $H_z(r,t)$, it is convenient to express equation (27) in terms of Cartesian coordinates, noting that values of H_z for positions along the axis of the cylinder correspond to $x=0$ where $\varphi=\pm\pi/2$ for $y>0$ or $y<0$, respectively. Also for positions along the axis of the cylinder, the coordinate z is fixed at $z=z_0$. We have then,

$$r=\sqrt{z_0^2+y^2}$$

$$\theta=\pi-\tan^{-1}\left(\frac{|y|}{z_0}\right)$$

$$\varphi=\pm\pi/2 \quad \text{FOR} \quad y>0 \quad \text{OR} \quad y<0$$

so that equation (27) becomes for $\varphi = +\pi/2$ and $y > 0$

$$\left(\frac{H_z}{H_0}\right)_{\varphi=+\frac{\pi}{2}} = \frac{2}{\pi}\left\langle -\left(\frac{r_0}{\sqrt{z_0^2+y^2}}\right)^3 \sin\left[\pi - \tan^{-1}\left(\frac{|y|}{z_c}\right)\right]\cos\left[\pi - \tan^{-1}\left(\frac{|y|}{z_c}\right)\right]\right.$$

$$+\frac{1}{5}\left(\frac{r_c}{\sqrt{z_c^2+y^2}}\right)^5\left\{\left(\frac{7}{8}\cos\left[\pi-\tan^{-1}\left(\frac{|y|}{z_0}\right)\right]\right)\left(5\sin 3\left[\pi-\tan^{-1}\left(\frac{|y|}{z_c}\right)\right]+\sin\left[\pi-\tan^{-1}\left(\frac{|y|}{z_c}\right)\right]\right)\right.$$

(34)

$$\left.\left. -2\sin 2\left[\pi-\tan^{-1}\left(\frac{|y|}{z_c}\right)\right]\right\}\right.$$

$$-\frac{1}{7}\left(\frac{r_0}{\sqrt{z_c^2+y^2}}\right)^7\left\{\left(\frac{33}{128}\cos\left[\pi-\tan^{-1}\left(\frac{|y|}{z_0}\right)\right]\right)\left(21\sin 5\left[\pi-\tan^{-1}\left(\frac{|y|}{z_0}\right)\right]+7\sin 3\left[\pi-\tan^{-1}\left(\frac{|y|}{z_c}\right)\right]\right.\right.$$

$$\left.\left.\left.+2\sin\left[\pi-\tan^{-1}\left(\frac{|y|}{z_0}\right)\right]\right)-\frac{3}{8}\left(7\sin 4\left[\pi-\tan^{-1}\left(\frac{|y|}{z_0}\right)\right]+2\sin 2\left[\pi-\tan^{-1}\left(\frac{|y|}{z_c}\right)\right]\right)\right\}\ldots\right\rangle$$

In numerical evaluation only the terms indicated in (34) are used in that the series converges rapidly for $r = \sqrt{z_0^2+y^2} > r_0$.

The experimental results and theoretical values obtained from equation (34) are given in Figure (5). Only $y > 0$ is shown in the figure; however, equation (27) yields directly

(35) $$\left(\frac{H_z}{H_0}\right)_{\varphi=-\frac{\pi}{2}} = -\left(\frac{H_z}{H_0}\right)_{\varphi=+\frac{\pi}{2}}$$

for $y < o$ and the experimental results also exhibit this odd symmetry in φ . The results in Figure (5) represent the sealing of the interior field at any particular point in time for which $H_o(t)$ and thus $H_z(\bar{r},t)$ have values, however, the experimental values shown are for the peak $H_z(\bar{r},t)$ values and peak $H_o(t)$ value. Peak values of the experimental results were used simply because these values can be read more accurately from the oscillograms than other values.

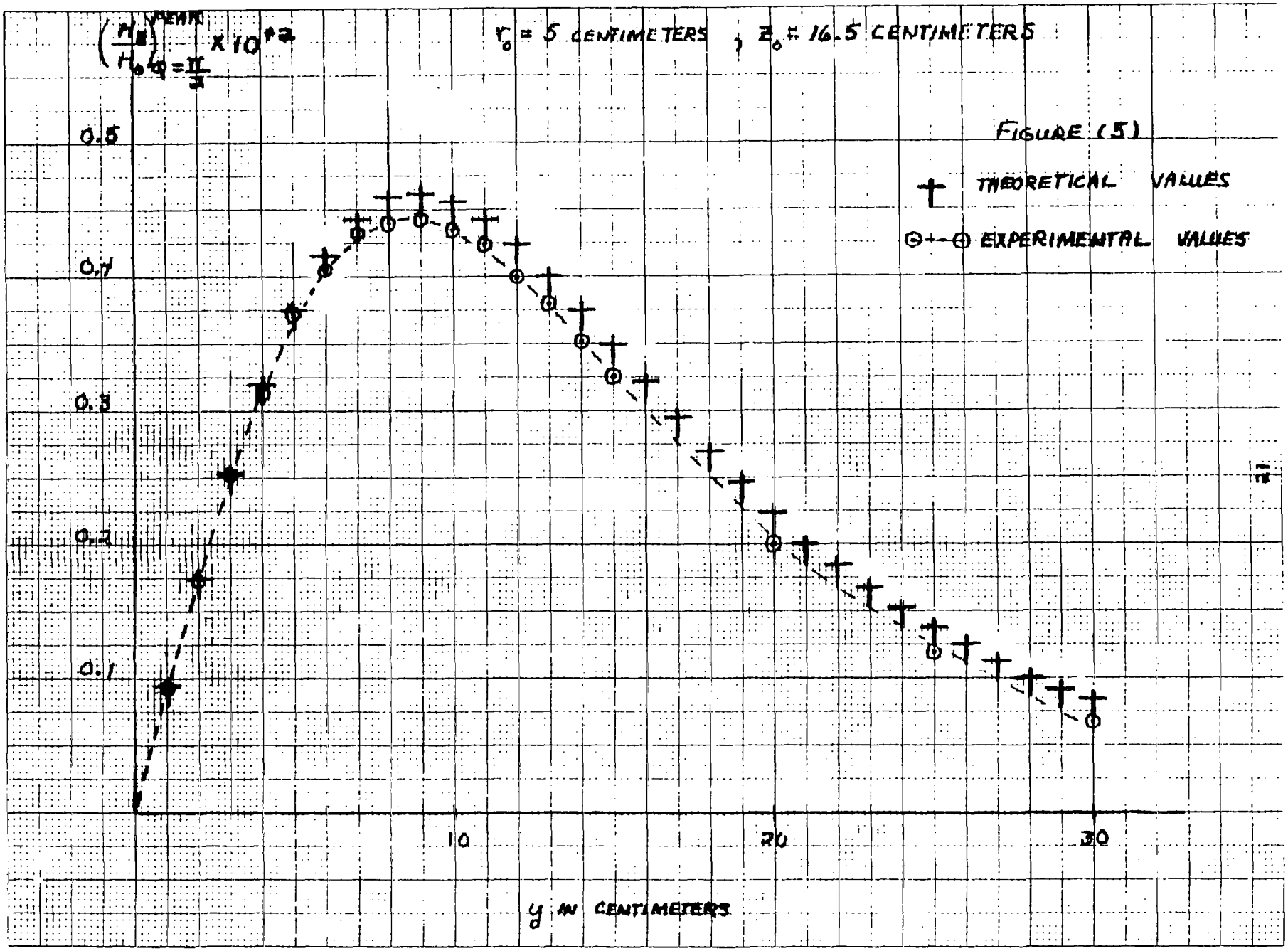
$\left(\frac{H_\theta}{H_0}\right)_{\theta=\frac{\pi}{2}}$ x 10^+2
r_0 = 5 CENTIMETERS , z_0 = 16.5 CENTIMETERS
FIGURE (5)
THEORETICAL VALUES
EXPERIMENTAL VALUES
0.5
0.4
0.3
0.2
0.1
10
20
30
y IN CENTIMETERS

IV. MULTIPLE APERTURES AND LINEAR SUPERPOSITION

We again consider an infinitely conducting plane of infinite extent with a vanishingly small thickness in which several circular apertures are located. The apertures need not be of the same radius, but each aperture's diameter must be small compared to wavelengths present in the external field. If we assume proximity effects are minimal for long wavelengths and small apertures, the most straightforward approximation to the problem is that of superposition of the individual aperture solutions. In Figure (6) below, we consider two apertures and desire the magnetic field at a point P :

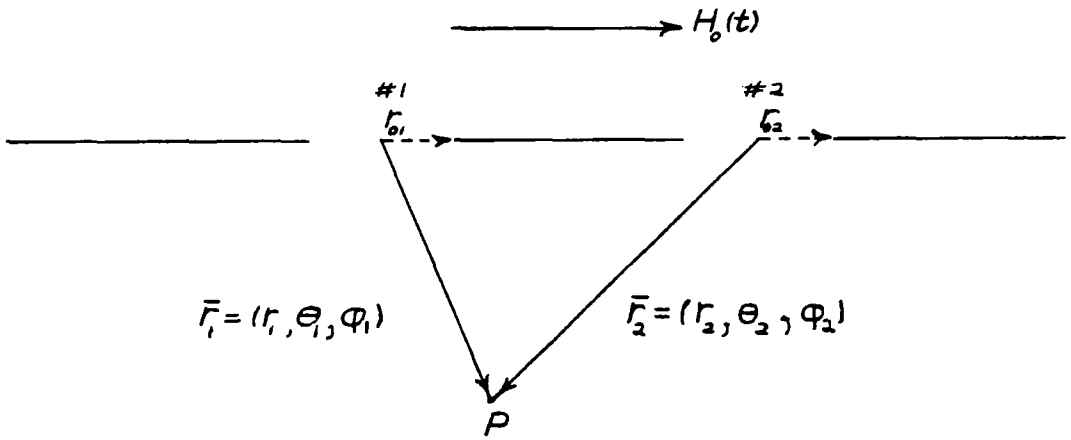

FIGURE (6)

In the above approximation, we take the field at the point P to be the sum of the fields due to aperture #1 in the absence of #2 at $\bar{r}_1$,

and due to aperture #2 in the absence of #1 at $\bar{r}_2$. In this manner any number of apertures can be treated approximately by superimposing the individual solutions. To test the approximation we consider now a two aperture experiment and the correlation of experimental and theoretical results.

V. TWO APERTURE EXPERIMENT AND CORRELATION FOR H_z

The external field illustrated in Figure (2) and given by equation (29) was employed again in the two aperture experiment. Also the geometry employed was the $\frac{1}{3}$ meter diameter aluminum cylinder used previously with a wall thickness of about $\frac{3}{16}$ inch. Two circular apertures both of 10 centimeter diameter were introduced on the lateral surface of the cylinder with a center to center axial spacing of 25 centimeters. The geometry of the experiment is illustrated below in Figure (7):

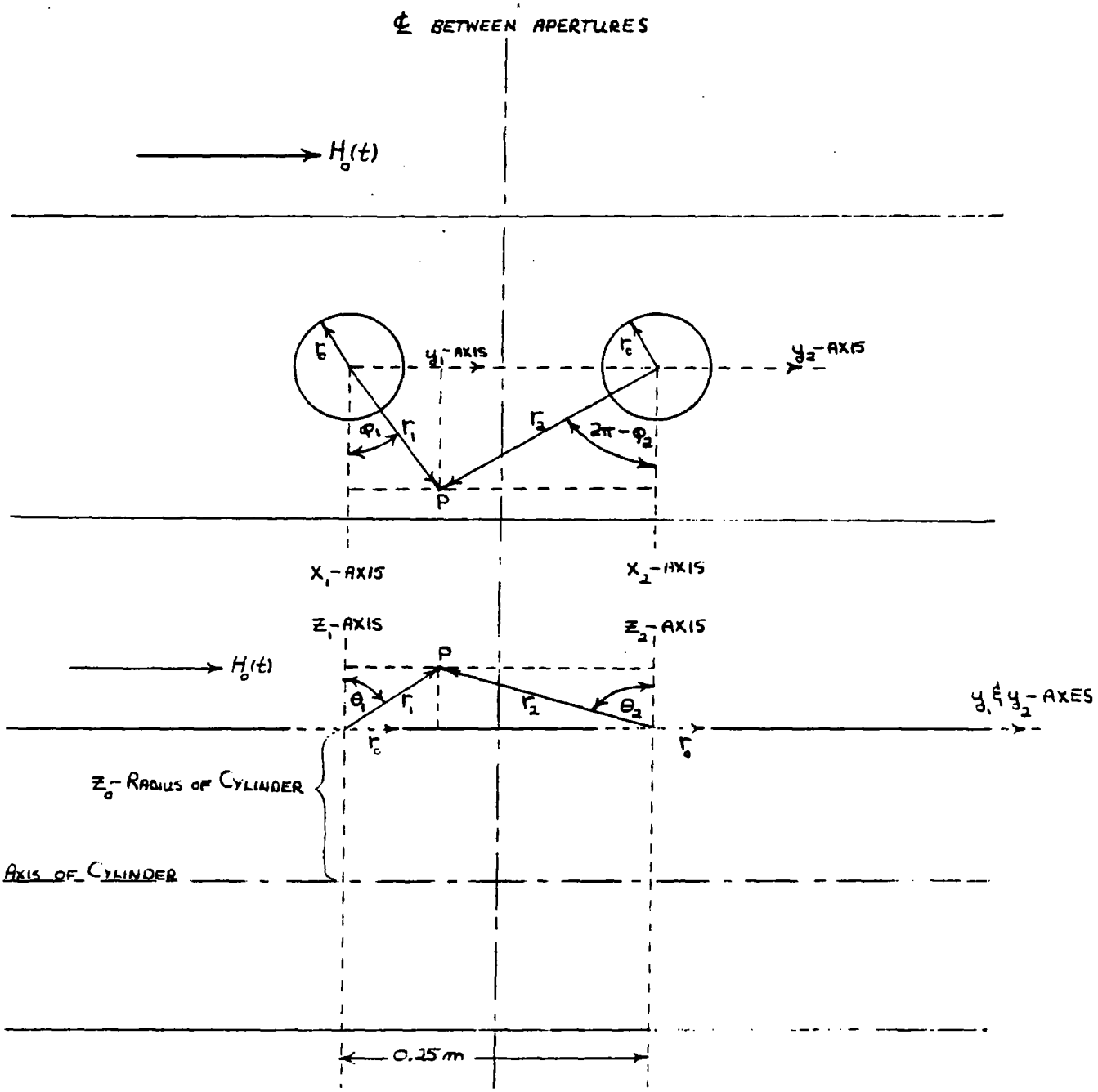
℄ BETWEEN APERTURES
$H_o(t)$
r_c
y_1-AXIS
r_c
y_2-AXIS
φ_1
r_1
r_2
$2\pi - \varphi_2$
P
X_1-AXIS
X_2-AXIS
Z_1-AXIS
Z_2-AXIS
$H_o(t)$
P
θ_1
r_1
r_2
θ_2
y_1 & y_2-AXES
r_c
r_o
Z_o- RADIUS OF CYLINDER
AXIS OF CYLINDER
0.25 m

FIGURE (7)

Time history measurements were made of the $H_z(\bar{r},t)$ field inside the cylinder at points along the axis of the cylinder. As in the one aperture experiment, the time history of the $H_z(\bar{r},t)$ measurements is the same as the time history for the external field, $H_o(t)$. We now apply quasistatic theory and the superposition approximation to obtain the field scaling. Applying equation (34) and the relation (35) to both apertures, we obtain the results shown in Figure (8). Now, choosing the intersection of the center line between the two apertures, shown in the lower part of Figure (7), with the y_1 , and y_2- axes as an origin, the theoretical solutions can be added and plotted about this origin. The theoretical and experimental values obtained are given in Figure (9).

In conclusion, I would like to thank Mr. Ronald Bostak and Mr. George Crowson for engineering support and the measurements taken in the above considered experiments.

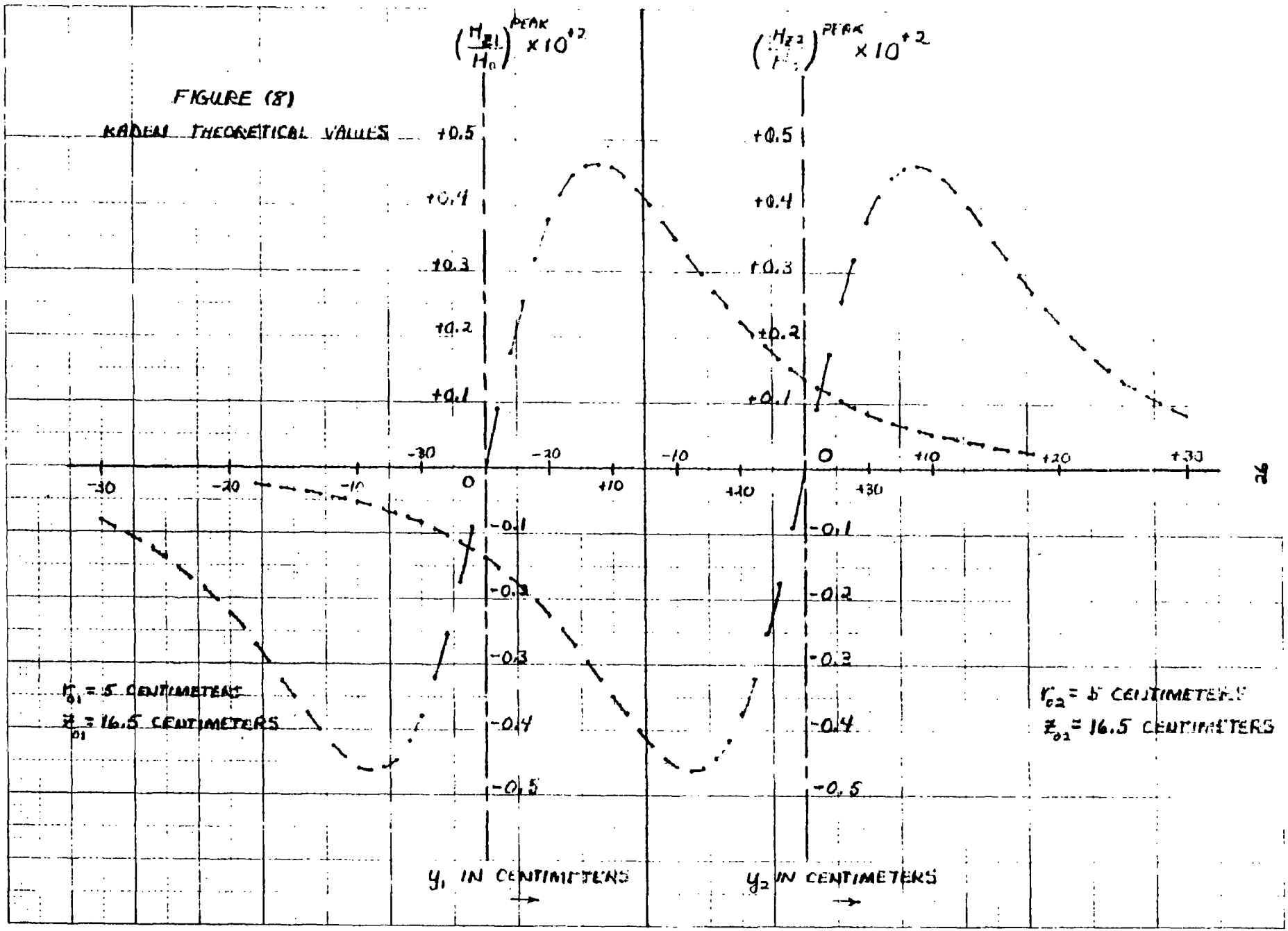
FIGURE (8)
RADIAL THEORETICAL VALUES
$\left(\frac{H_{z1}}{H_0}\right)^{PEAK} \times 10^{+2}$
$\left(\frac{H_{z2}}{H_0}\right)^{PEAK} \times 10^{+2}$
+0.5
+0.4
+0.3
+0.2
+0.1
-0.1
-0.2
-0.3
-0.4
-0.5
-30
-20
-10
0
+10
+20
+30
r_{01} = 5 CENTIMETERS
z_{01} = 16.5 CENTIMETERS
r_{02} = 5 CENTIMETERS
z_{02} = 16.5 CENTIMETERS
y_1 IN CENTIMETERS
y_2 IN CENTIMETERS

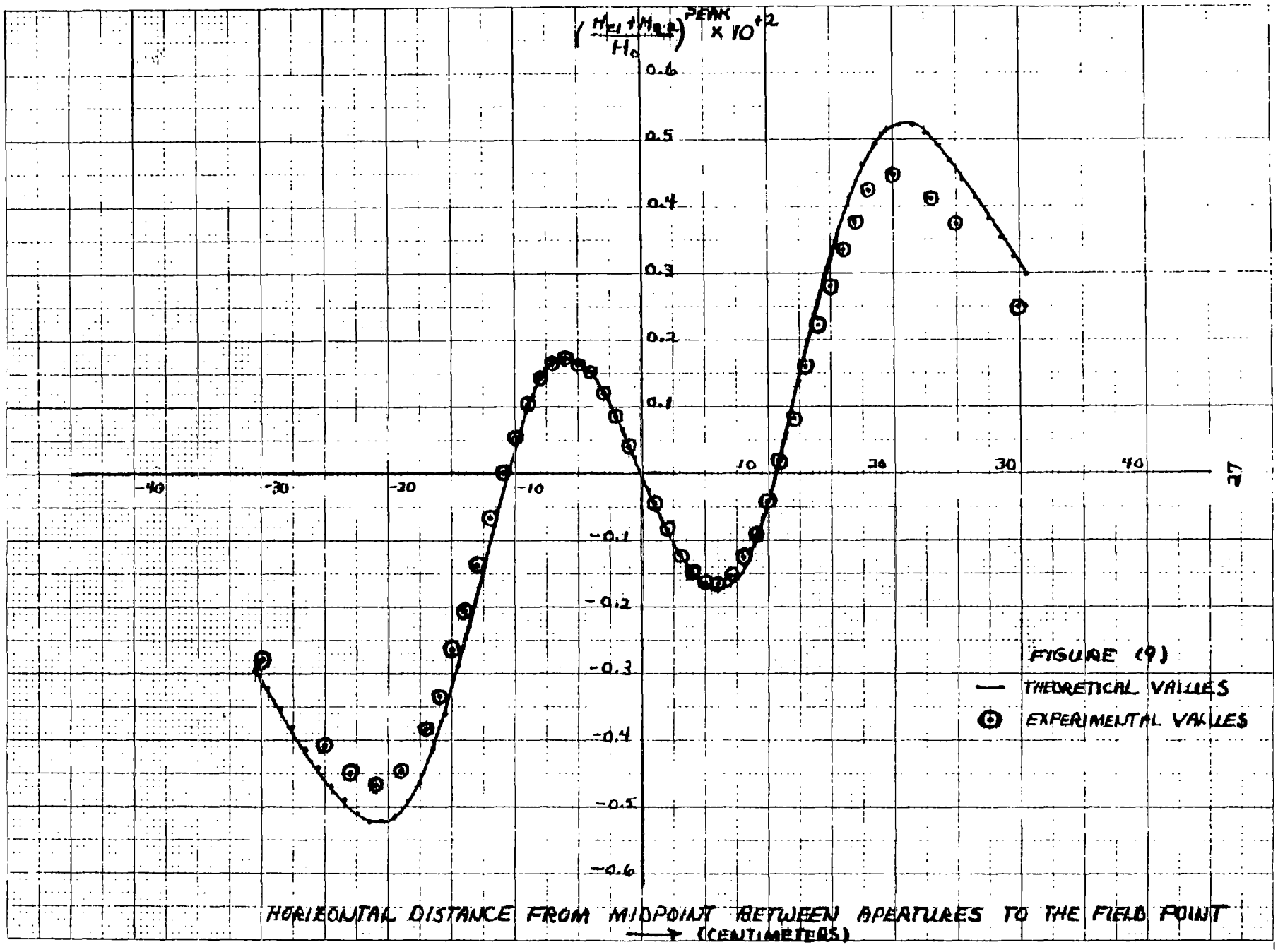
$\left(\frac{H_{e1}+H_{e2}}{H_0}\right)^{PEAK} \times 10^{+2}$
0.6
0.5
0.4
0.3
0.2
0.1
-0.1
-0.2
-0.3
-0.4
-0.5
-0.6
-40
-30
-20
-10
10
20
30
40
27
FIGURE (9)
THEORETICAL VALUES
EXPERIMENTAL VALUES
HORIZONTAL DISTANCE FROM MIDPOINT BETWEEN APERTURES TO THE FIELD POINT
(CENTIMETERS)

APPENDIX

To obtain the Cartesian components of the magnetic field, we have first for H_x ,

$$H_x = \frac{2H_0 \sin\theta \sin\varphi \cos\varphi}{\pi} \sum_{m=1,3,5,\ldots}^{\infty} \frac{(-1)^{(m-1)/2}}{m(m+2)} (m+1) \left(\frac{r_0}{r}\right)^{m+2} P_m^1(\cos\theta)$$

$$- \frac{2H_0 \cos\theta \sin\varphi \cos\varphi}{\pi \sin\theta} \sum_{m=1,3,5,\ldots}^{\infty} \frac{(-1)^{(m-1)/2}}{m(m+2)} \left(\frac{r_0}{r}\right)^{m+2} \left[m\cos\theta P_m^1(\cos\theta) - (m+1) P_{m-1}^1(\cos\theta)\right]$$

$$+ \frac{2H_0 \sin\varphi \cos\varphi}{\pi \sin\theta} \sum_{m=1,3,5,\ldots}^{\infty} \frac{(-1)^{(m-1)/2}}{m(m+2)} \left(\frac{r_0}{r}\right)^{m+2} P_m^1(\cos\theta),$$

or

$$H_x = \frac{2H_0 \sin\varphi \cos\varphi}{\pi} \left\{ \sin\theta \sum_{m=1,3,5,\ldots}^{\infty} \frac{(-1)^{(m-1)/2}}{m(m+2)} \left(\frac{r_0}{r}\right)^{m+2} (m+1) P_m^1(\cos\theta) \right.$$

$$- \frac{\cos\theta}{\sin\theta} \sum_{m=1,3,5,\ldots}^{\infty} \frac{(-1)^{(m-1)/2}}{m(m+2)} \left(\frac{r_0}{r}\right)^{m+2} \left[m\cos\theta P_m^1(\cos\theta) - (m+1) P_{m-1}^1(\cos\theta)\right]$$

$$\left. + \frac{1}{\sin\theta} \sum_{m=1,3,5,\ldots}^{\infty} \frac{(-1)^{(m-1)/2}}{m(m+2)} \left(\frac{r_0}{r}\right)^{m+2} P_m^1(\cos\theta) \right\}.$$

Collecting terms, we have

$$H_x = \frac{2H_0 \sin\varphi \cos\varphi}{\pi} \left\{ \sum_{m=1,3,5,\ldots}^{\infty} \frac{(-1)^{(m-1)/2}}{m(m+2)} \left(\frac{r_0}{r}\right)^{m+2} \left[(m+1)\sin\theta P_m^1(\cos\theta) \right.\right.$$

$$\left.\left. - \frac{m\cos^2\theta}{\sin\theta} P_m^1(\cos\theta) + \frac{(m+1)\cos\theta}{\sin\theta} P_{m-1}^1(\cos\theta) + \frac{1}{\sin\theta} P_m^1(\cos\theta) \right] \right\}$$

and thus

$$H_x = \frac{2H_0 \sin\varphi\cos\varphi}{\pi}\left\{\sum_{m=1,3,5,\ldots}^{\infty}\frac{(-1)^{(m-1)/2}}{m(m+2)}\left(\frac{r_c}{r}\right)^{m+2}\left[P_m^1(\cos\theta)\left((m+1)\sin\theta+\frac{1-m\cos^2\theta}{\sin\theta}\right)\right.\right.$$

$$\left.\left.+\frac{(m+1)\cos\theta}{\sin\theta}P_{m-1}^1(\cos\theta)\right]\right\}.$$

In a similar manner, we have for H_y ,

$$H_y = \frac{2H_0\sin^2\varphi\sin\theta}{\pi}\sum_{m=1,3,5,\ldots}^{\infty}\frac{(-1)^{(m-1)/2}(m+1)}{m(m+2)}\left(\frac{r_c}{r}\right)^{m+2}P_m^1(\cos\theta)$$

$$-\frac{2H_0\sin^2\varphi\cos\theta}{\pi\sin\theta}\sum_{m=1,3,5,\ldots}^{\infty}\frac{(-1)^{(m-1)/2}}{m(m+2)}\left(\frac{r_c}{r}\right)^{m+2}\left[m\cos\theta\,P_m^1(\cos\theta)-(m+1)P_{m-1}^1(\cos\theta)\right]$$

$$-\frac{2H_0\cos^2\varphi}{\pi\sin\theta}\sum_{m=1,3,5,\ldots}^{\infty}\frac{(-1)^{(m-1)/2}}{m(m+2)}\left(\frac{r_c}{r}\right)^{m+2}P_m^1(\cos\theta)$$

or

$$H_y = \frac{2H_0}{\pi}\left\{\sum_{m=1,3,5,\ldots}^{\infty}\frac{(-1)^{(m-1)/2}}{m(m+2)}\left(\frac{r_c}{r}\right)^{m+2}P_m^1(\cos\theta)(m+1)\sin^2\varphi\sin\theta\right.$$

$$-\sum_{m=1,3,5,\ldots}^{\infty}\frac{(-1)^{(m-1)/2}}{m(m+2)}\left(\frac{r_c}{r}\right)^{m+2}\frac{\sin^2\varphi\cos\theta}{\sin\theta}\left[m\cos\theta\,P_m^1(\cos\theta)-(m+1)P_{m-1}^1(\cos\theta)\right].$$

$$\left.-\sum_{m=1,3,5,\ldots}^{\infty}\frac{(-1)^{(m-1)/2}}{m(m+2)}\left(\frac{r_c}{r}\right)^{m+2}\frac{\cos^2\varphi}{\sin\theta}P_m^1(\cos\theta)\right\}.$$

Collecting terms, we have

$$H_y = \frac{2H_0}{\pi}\left\{\sum_{m=1,3,5,\ldots}^{\infty}\frac{(-1)^{(m-1)/2}}{m(m+2)}\left(\frac{r_c}{r}\right)^{m+2}\left(P_m^1(\cos\theta)\left[(m+1)\sin^2\varphi\sin\theta\right.\right.\right.$$

$$\left.\left.\left.-\frac{m\sin^2\varphi\cos^2\theta}{\sin\theta}-\frac{\cos^2\varphi}{\sin\theta}\right]+(m+1)P_{m-1}^1(\cos\theta)\right)\right\}$$

and thus

$$H_y = \frac{2H_o}{\pi}\left\{\sum_{m=1,3,5,\ldots}^{\infty} \frac{(-1)^{(m-1)/2}}{m(m+2)}\left(\frac{r_o}{r}\right)^{m+2}\left[P_m^1(\cos\theta)\left((m+1)\sin^2\varphi\sin\theta - \frac{m\sin^2\varphi\cos^2\theta+\cos^2\varphi}{\sin\theta}\right) + (m+1)P_{m-1}^1(\cos\theta)\right]\right\}.$$

Lastly, we have for H_z,

$$H_z = \frac{2H_o\sin\varphi\cos\theta}{\pi}\sum_{m=1,3,5,\ldots}^{\infty} \frac{(-1)^{(m-1)/2}}{m(m+2)}\left(\frac{r_o}{r}\right)^{m+2}(m+1)P_m^1(\cos\theta)$$

$$+ \frac{2H_o\sin\varphi}{\pi}\sum_{m=1,3,5,\ldots}^{\infty} \frac{(-1)^{(m-1)/2}}{m(m+2)}\left(\frac{r_o}{r}\right)^{m+2}\left[m\cos\theta P_m^1(\cos\theta) - (m+1)P_{m-1}^1(\cos\theta)\right]$$

or

$$H_z = \frac{2H_o\sin\varphi}{\pi}\left\{\sum_{m=1,3,5,\ldots}^{\infty} \frac{(-1)^{(m-1)/2}}{m(m+2)}\left(\frac{r_o}{r}\right)^{m+2}\left[P_m^1(\cos\theta)\{(m+1)\cos\theta + m\cos\theta\} - (m+1)P_{m-1}^1(\cos\theta)\right]\right\}$$

and thus

$$H_z = \frac{2H_o\sin\varphi}{\pi}\left\{\sum_{m=1,3,5,\ldots}^{\infty} \frac{(-1)^{(m-1)/2}}{m(m+2)}\left(\frac{r_o}{r}\right)^{m+2}\left[(2m+1)\cos\theta P_m^1(\cos\theta) - (m+1)P_{m-1}^1(\cos\theta)\right]\right\}.$$

VI. LIST OF REFERENCES

1. HEINRICH KADEN, WIRBELSTROME UND SCHIRMUNG IN DER NACHAICNTENTECHNIK, TECHNISCHE PHYSIK IN EINZELDARSTELLUNGEN 10, SPRINGER-VERLAG, 1959.

2. JOHN N. BOMBARDT, JR., "MAGNETIC FIELD SHIELDING DEGRADATION DUE TO CIRCULAR APERTURES IN LONG HOLLOW CYLINDERS", EMP INTERACTION NOTES - NOTE III, AIR FORCE WEAPONS LABORATORY, 21 SEPTEMBER 1966.